



Published in final edited form as:

*J Endod.* 2018 May ; 44(5): 806–812. doi:10.1016/j.joen.2017.12.003.

## Novel Endodontic Disinfection Approach Using Catalytic Nanoparticles.

**Sarah Bukhari, B.D.S, M.S.,**

Dept. of Endodontics, School of Dental Medicine, University of Pennsylvania.

**Dongyeop Kim, P.h.D.,**

School of Dental Medicine, University of Pennsylvania.

**Yuan Liu, DDS, P.h.D.,**

School of Dental Medicine, University of Pennsylvania.

**Bekir Karabucak, D.M.D, M.S.,** and

Dept. of Endodontics, School of Dental Medicine, University of Pennsylvania., 240 S. 40th Street, Philadelphia, PA. 19104.

**Hyun Koo, D.D.S, M.S, PhD.**

Dept. of Orthodontics and Divisions of Pediatric Dentistry & Community Oral Health, School of Dental Medicine, University of Pennsylvania.

### Abstract

**Introduction:** The aim of the study was to test a new disinfection technology using biomimetic iron oxide nanoparticles (IO-NP) with peroxidase-like activity to enhance antibacterial activity on root canal surfaces and in dentinal tubules.

**Materials and Methods:** Canal surfaces and dentinal tubules of single rooted intact extracted teeth were infected by growing *Enterococcus faecalis* biofilms for three weeks. The samples were divided into 6 treatment groups: 1) PBS (negative control), 2) 3% H<sub>2</sub>O<sub>2</sub>, (test control), 3) IO-NP (0.5 mg/ml) (test control), 4) IO-NP (0.5 mg/ml) + 3% H<sub>2</sub>O<sub>2</sub>, 5) 3% NaOCl, (positive control), and 6) 2% CHX, (positive control). Environmental Scanning Electron Microscopy coupled with Energy Dispersive Spectroscopy was used to confirm IO-NP binding to the canal surface after a single treatment. Specimens were labeled with fluorescent staining for live/dead cells and Confocal Laser Scanning Microscopy was used for quantification of dead bacteria relative to the negative control (PBS).

**Results:** Both biofilm formation and dentinal tubules infection were successfully recapitulated using the in vitro model. IO-NP was capable of binding to the infected canal surfaces despite a

---

**Corresponding author** Bekir Karabucak, D.M.D., M.S., Dept. of Endodontics, School of Dental Medicine, University of Pennsylvania., 240 S. 40th Street, Philadelphia, PA. 19104., bekirk@upenn.edu.

The authors deny any conflicts of interest related to this study.

**Publisher's Disclaimer:** This is a PDF file of an unedited manuscript that has been accepted for publication. As a service to our customers we are providing this early version of the manuscript. The manuscript will undergo copyediting, typesetting, and review of the resulting proof before it is published in its final citable form. Please note that during the production process errors may be discovered which could affect the content, and all legal disclaimers that apply to the journal pertain.

single, short-term (5 min) treatment. IO-NP activation of H<sub>2</sub>O<sub>2</sub> killed significantly more *E. faecalis* present on canal surfaces and at different depth of dentinal tubules when compared to all other experimental groups ( $P < 0.05$ – $0.0005$ ).

**Conclusion:** The results reveal the potential to exploit nanocatalysts with enzyme-like activity as a potent alternative approach for the treatment of endodontic infections.

---

## INTRODUCTION

The role of microorganisms as the primary cause of apical periodontitis has been well established (1), and thereby efforts have been directed towards eliminating them for higher success in Endodontics (2). The disinfection process is challenging due to the complexity of the root canal system and the presence of isthmuses, accessory canals, and dentinal tubules, all of which can harbor bacteria and biofilms (3). Several studies have demonstrated the presence of biofilm inside the root canal (4,5) with bacterial penetration of dentinal tubules at varying depth (6,7).

The mechanical preparation can physically remove tissue remnants, biofilms and infected dentin (8). However, large portions of the root canal system following mechanical preparation may remain un-instrumented (9,10). Although current chemical irrigants, such as chlorhexidine and NaOCl, are effective antimicrobials, they are still incapable of eradicating bacterial infection with limited efficacy to completely disinfect dentinal tubules (11,12).

Advances in nanotechnology have provided new and promising opportunities to kill bacteria, disrupt biofilm and control dentinal tubules infection (13,14). A wide range of nanoparticles (NPs) with antimicrobial activity has been developed including inorganic (particularly silver) and chitosan-based NPs. Although these nanoparticles are potentially effective technology for endodontic disinfection, the prolonged contact time required to achieve effective bacterial killing as well as toxicity issues in case of silver NPs imposes significant drawbacks (13). Nevertheless, newer nanoparticle formulations as well as other technologies (such as photodynamic therapy) have been reported to enhance biofilm elimination (13, 15).

Iron oxide nanoparticles have been widely used as contrast agents in MRI because of their high biocompatibility and ability to penetrate tumor and atherosclerotic plaque, resulting in many FDA-approved formulations. Recently, biocompatible iron oxide (Fe<sub>3</sub>O<sub>4</sub>) NPs (IO-NP) has shown to have potent anti-biofilm properties without deleterious effects on oral tissues *in vivo* (16). These nanoparticles possess an intrinsic peroxidase-like activity, which enables them to catalyze hydrogen peroxide (H<sub>2</sub>O<sub>2</sub>) to generate free radicals in a pH-dependent manner. H<sub>2</sub>O<sub>2</sub> is a commonly used disinfectant that displays antibacterial activity via free-radical generation, but the process is slow with limited anti-biofilm effects when used alone (17). Iron oxide nanocatalysts can potentiate the antibiofilm efficacy of H<sub>2</sub>O<sub>2</sub>. The IO-NPs retained within the biofilm following topical treatment can rapidly catalyze H<sub>2</sub>O<sub>2</sub> at acidic pH generating free-radicals and killing the embedded bacteria within minutes, resulting in an effective and biocompatible treatment *in vivo* (16,18).

Considering the complex endodontic environment and difficulty of penetrating dentinal tubules, there is a potential opportunity to exploit nanocatalysts as a feasible therapeutic approach against biofilm infection of the root canal. Therefore, the aim of the study was to test whether catalytic iron oxide nanoparticles can be used as new endodontic disinfection technology to enhance antibacterial activity on root canal surfaces and in dentinal tubules.

## MATERIALS & METHODS

Single rooted intact extracted teeth were used in this study. Each tooth was horizontally sectioned at 1 mm level below the cemento-enamel junction to produce a 4 mm dentin blocks. The canals were enlarged to size 6 Gates Glidden drill (1.5 mm in diameter). Each dentin block was split into 2 semi-cylindrical halves. The outer surfaces of each half were ground to achieve a standard thickness of 2 mm and to remove the root surface cement. Each specimen was treated with 5.25% NaOCl followed by 17% EDTA for 4 minutes using an ultrasonic bath for smear layer removal. Samples were rinsed in sterile water for 10 minutes thereafter to eliminate any residual chemicals. Specimens were then sterilized by autoclave for 20 minutes at 121°C. (Figure 1)

The clinical strain *E. faecalis* OG1RF isolated from retreatment cases (gift from Dr. Brenda Gomes, State University of Campinas) was used as a test organism for this study. Isolated colonies of pure *E. faecalis* culture grown in blood agar were suspended in BHI (Dot Scientific, Inc. Burton, MI, USA) and incubated overnight. Five hundred microliters of the bacterial suspension was re-suspended in BHI and standardized spectrophotometrically to an optical density of 0.5 absorbance at 600 nm (OD<sub>600</sub> = 0.5). Five hundred microliters of the adjusted *E. faecalis* suspension was then added to each well (Olympus 24 well plate, 3.5 ml, Genesee Scientific. San Diego, CA, USA) containing 2 ml of fresh BHI medium and the dentin specimen (Figure 1). All samples were then incubated at 37°C for 3 weeks. Medium was changed every 48h.

The infected root dentin blocks were rinsed in sterile water for one minute and transferred to cell culture wells. The outer surface of the specimens was covered with nail varnish, and then randomly divided into 6 treatment groups: 1) PBS (negative control), 2) 3% H<sub>2</sub>O<sub>2</sub>, 3) IO-NP (0.5 mg/ml; dosage based on previous study, (16)), 4) IO-NP (0.5 mg/ml)<sub>-</sub> + 3% H<sub>2</sub>O<sub>2</sub> (IO-NP/H<sub>2</sub>O<sub>2</sub>; 'new irrigant'), 5) 3% NaOCl and 6) 2% CHX. For the 'new irrigant' test solution, 50 µl of IO-NP was placed on the infected surface of the root canal for 5 minutes. Then, the excess IO-NP solution was washed with sterile water and 50µl of 3% H<sub>2</sub>O<sub>2</sub> was placed for additional 5 minutes. For all others, each irrigation solution (50µl) was placed as described above for 5 minutes, then treated with additional 5 minutes of sterile water to standardize the treatment time to a total of 10 minutes. After treatment, the specimens were vertically split through the root canal into 2 halves and longitudinally visible dentin tubules (Figure 1) were examined via confocal laser scanning microscopy.

Additional root dentin samples were prepared for SEM analysis. Two samples were examined to verify a successful smear layer removal, while 4 samples were used to verify biofilm formation on the canal surface and bacterial infection of dentinal tubules. For SEM examination, samples were fixed in 2.5% glutaraldehyde and 2.0% paraformaldehyde in

Author Manuscript

cacodylate buffer overnight at 4°C. After 3 series of phosphate buffer washes, the samples were post-fixed and dehydrated in a graded ethanol series. Then, the samples were treated with two changes of hexamethyldisilazane (HMDS) and allowed to air dry prior to mounting and sputter coating with gold/palladium. SEM images were acquired with an FEI Quanta FEG 250 SEM. To confirm IO-NP binding to the canal surfaces, two root dentin samples were topically treated with 0.5 mg/ml IO-NP for 5 minutes followed by washing for 1 minute with sterile water, and compared to two untreated specimens. FEI Quanta 600 FEG Environmental Scanning Electron Microscopy (ESEM) coupled with Energy Dispersive Spectroscopy (EDS) was used to visualize and identify IO-NP on treated samples. The EDS elemental analysis was performed to assess the spatial distribution of iron on the same image area taken by ESEM.

Author Manuscript

Author Manuscript

Confocal Laser Scanning Microscopy (CLSM) was used as an analytical tool to examine both bacterial viability and their distribution across the dentinal tubules length. This method can quantify the viability of bacteria after the use of different irrigants while providing information about the spatial distribution of infection. Following treatment, samples were stained with fluorescent LIVE/DEAD® Ba cLight™ Bacterial Viability kit (Molecular Probes, Eugene, OR) containing SYTO®9 green-fluorescent nucleic acid stain and the red-fluorescent nucleic acid stain, propidium iodide (PI). Each of the samples was initially rinsed with PBS for 1 minute and mounted on the microscope stage. Dentin surfaces were then examined using multi-photon Leica SP5 microscope (Leica Microsystems GmbH, Mannheim, Germany). Specimens were viewed with 20× LPlan (numerical aperture, 1.05) water immersion objective lens with no additional zoom. Samples were standardized to 2 mm in length (Figure 1.E) and dentin surface was divided into 3 zones: inner (the closest to canal lumen), middle and outer. Each zone was equivalent to 0.66 mm. The CLSM field of view was set at 0.77 × 0.77 mm (1/3 of the sample was viewed under the microscope), and the extra 0.1mm was utilized as a mark to determine the end of one zone and the beginning of the other. Each specimen was scanned at 6 positions (2/zone) randomly after determination of the zone (inner, middle or outer), and confocal image series were generated by optical sectioning at each of these positions. Forty-micrometer-deep scans (0.5-µm step size, 82 slices/ scan) were obtained at a resolution of 512×512 pixel. Amira 5.4.1 software (Visage Imaging, San Diego, CA) was used to create 2D images showing live/dead bacteria while ImageJ (<https://imagej.nih.gov/ij/>) was used to convert the fluorescence signal intensity from confocal image stacks into numerical values for quantitative analysis. In our experimental settings, the dentin autofluorescence overlapped with SYTO9 fluorescence signal, making a determination of viable cells unreliable. Therefore, we focussed on quantification of numerical values corresponding to dead bacteria (labeled by PI). To reduce any potential subjectivity from different levels of background noise in each scanning, the threshold was set by two independent examiners; threshold setting was also a blinded process to reduce bias. Then, the average values from the two examiners were obtained and the amount of total dead cells was calculated. All the data from each experimental group was normalized to PBS (negative control), and presented as fold-change (vs. PBS). The data were statistically analyzed using GraphPad Prism software version 5.0 (GraphPad Software Inc., San Diego, CA, USA). Two tailed unpaired t -test was used to compare two sets of data at a time at a significance level of P < 0.05.

## RESULTS

### Analysis of *E. faecalis* Infection and IO-NP Binding:

A successful removal of smear layer was observed via SEM, as dentinal tubules openings appear to be clear and unclogged. In the infected group, SEM analysis revealed bacterial clusters bound to the canal surface after 3 weeks of *E. faecalis* biofilm formation with bacterial cells extending into dentinal tubules. The spatial distribution of the *enterococci* along the tubules was also visualized, showing heavy infection at the inner zone closer to the canal lumen (Figure 2).

IO-NP was retained following short-term, topical application (5 minutes) akin to clinical situation for endodontic treatment. Small particles at nanometer scale were bound to the bacterial surface (Figure 2.D). In contrast, these particles were absent on the surfaces of untreated canal (Figure 2.C). EDS quantitative analysis further confirmed the presence of iron on IO-NP-treated surface (vs. no iron detection in buffer control-treated surface; Figure 2.E–2.F) and its distribution was mapped out (Figure 2.F1–2.F2), which correlated well with the IO-NP location observed in ESEM image. The data showed that the nanoparticles retained within the canal, while binding to the bacterial surface following a single, short-term topical treatment demonstrating its feasibility for endodontic treatment.

### Antibacterial Activity of IO-NP/ H<sub>2</sub>O<sub>2</sub>:

In order to understand the antimicrobial efficacy of nanoparticles, three dentinal tubule zones based on the distance from the root canal lumen were evaluated (Figure 3.A). Overall, IO-NP/ H<sub>2</sub>O<sub>2</sub> was more effective in killing *E. faecalis* in all 3 zones when compared to all other experimental groups ( $P < 0.05$ ; Figure 3.B). IO-NP/H<sub>2</sub>O<sub>2</sub> was several fold more effective in killing *E. faecalis* at the inner zone (>15-fold;  $P < 0.05$ ), at the middle zone (~ 40-fold;  $P < 0.05$ ) and at the outer zone (~ 7-fold;  $P < 0.05$ ) when compared to test controls H<sub>2</sub>O<sub>2</sub> or IO-NP.

Furthermore, the antibacterial activity of IO-NP/H<sub>2</sub>O<sub>2</sub> was significantly better than the conventional irrigants throughout the dentinal tubules length, particularly in the middle zone. IO-NP/ H<sub>2</sub>O<sub>2</sub> was >9-fold more effective at the inner zone, while showing ~ 30-fold more *E. faecalis* killing at the middle zone when compared to CHX or NaOCl ( $P < 0.05$ ). IO-NP/H<sub>2</sub>O<sub>2</sub> also exhibited better antibacterial activity at the outer zone (~5-fold more killing vs. CHX or NaOCl;  $P < 0.05$ ). CHX or NaOCl displayed significant antibacterial activity compared to negative control ( $P < 0.0005$ ) and they were both significantly more effective than H<sub>2</sub>O<sub>2</sub> alone in all zones ( $P < 0.05$ ), except the outer surface in the NaOCl group. In contrast, there were no significant differences in bacterial killing efficacy between CHX and NaOCl.

## DISCUSSION

Microbial infection of the root canal has been implicated as the primary cause of apical periodontitis (1) by forming pathogenic biofilms (5,19). Furthermore, infection within the dentinal tubules has been reported to occur in 70% to 80% of the teeth with primary apical periodontitis and may be associated with endodontic treatment failure (20,21). NaOCl is considered the 'gold standard' endodontic irrigant (22), yet it has been reported that 40%

–60% of root canals still harbor viable bacteria after irrigation (23). Chlorhexidine has been also shown to have a comparable antimicrobial effect to NaOCl (26). However, both irrigants have demonstrated reduced efficacy for dentinal tubules disinfection, with antibacterial activity limited to the superficial layers of the dentin (11). Hence, new approaches are needed as optimal dentin disinfection could help maximize a successful treatment outcome. In an attempt to address these challenges, we proposed to use IO-NP in combination with H<sub>2</sub>O<sub>2</sub> as a new strategy to disinfect dentinal tubules more effectively than current modalities. IO-NP/H<sub>2</sub>O<sub>2</sub> displayed a strong antimicrobial activity against *E. faecalis* infection of dentinal tubules, which was significantly superior to CHX and NaOCl especially at the middle and outer zones. The excellent disinfection capacity was achieved due to IO-NP activation of H<sub>2</sub>O<sub>2</sub> through its intrinsic ‘peroxidase-like activity’ catalyzing free radicals generation on site that rapidly kills bacteria (16).

The mechanism of action is based on iron oxide-mediated ‘nanocatalysis’ whereby H<sub>2</sub>O<sub>2</sub> binds into the iron oxide nanostructure with subsequent activation of H<sub>2</sub>O<sub>2</sub> by ferric and ferrous ions in situ, generating free radicals ·OH (hydroxyl radical) and O<sub>2</sub><sup>·-</sup>/HO<sub>2</sub><sup>·</sup> (superoxide anion radical/perhydroxyl radical) (13). Importantly, this mechanism was found to be pH dependent, so that the catalysis is activated at acidic pH (between 4.5–5.5) but abolished at physiological pH above 7.0 (25) The pH-dependent functionality prevents catalytic reaction at physiological pH and unmitigated free-radical production, thereby providing a biocompatible treatment *in vivo* (16, 18). Excitingly, IO-NP/H<sub>2</sub>O<sub>2</sub> displayed potent antimicrobial effects across the entire tubule length, and it was more effective in killing *E. faecalis* when compared to NaOCl and CHX. IO-NP and H<sub>2</sub>O<sub>2</sub> were also tested to examine the antimicrobial effect of either of them when used alone. As expected, IO-NP or H<sub>2</sub>O<sub>2</sub> alone showed modest effects, supporting the mechanism by which IO-NP/ H<sub>2</sub>O<sub>2</sub> combination for optimal *E. faecalis* killing though nanocatalysis.

It is important to note that several other nanoparticles have been tested for antimicrobial purposes in root canal treatment (13,14). Nanoparticles could be of a great value due to their nanoscale size that results in a significant increase of their surface area and theoretically enables them to penetrate dentinal tubules which have a diameter ranging between 2.4 to 2.9 μm (26). Silver nanoparticles have been the most widely investigated as an antimicrobial in endodontic infections. It was found to be as effective as 5.25% NaOCl against *E. faecalis* and *Staphylococcus aureus*, helping to control the bacterial growth in the intracanal environment (27). However, prolonged contact time with bacteria is required for effective eradication, which was stated as a good option for intracanal medicament but a weak irrigant (28) in addition to potential cytotoxicity against mammalian cells. Chitosan nanoparticles are biocompatible, but similarly prolonged contact time is required for effective bacterial elimination (13,14). Our results show that a single IO-NP/H<sub>2</sub>O<sub>2</sub> treatment with 5-minute exposure time was substantially more effective than current irrigants. Thus, IO-NP/H<sub>2</sub>O<sub>2</sub> could be potentially more effective than existing modalities, although a direct comparison needs to be conducted *in vivo*.

A single species infection model with *E. faecalis* was used in this *in vitro* study. Although endodontic infection is polymicrobial, *E. faecalis* strain has been selected because of their frequent isolation from a persistent case of apical periodontitis (29) and its ability to invade

DT (30). Furthermore, *E. faecalis* has been shown to survive high pH levels (31), starvation and entombment (32). However, future studies should be directed toward building multispecies model that better recapitulate the complex nature of endodontic infections as well as testing IO-NP/H<sub>2</sub>O<sub>2</sub> antimicrobial efficacy in these models. Another limitation of this study is, the volume of irrigant used (50µl), which does not reflect the typical amount used in clinical practice. This is important, as the irrigant volume and the effect of fluid flow influence the canal cleanliness and irrigant efficacy (33). In addition, there is a limitation of using only one technique to assess disinfection. Although microbial culturing of dentin samples has been traditionally used to assess bacteria viability and disinfection efficacy (30), these methods (albeit quantitative) provide little information about the spatial distribution of cell viability across DT, an important aspect of our disinfection system using catalytic nanoparticles. In an effort to overcome the shortcomings of aforementioned methodology, a CLSM-based approach has been developed that allows quantitative analysis and visualization of the spatial distribution of bacteria within the infected dentin and dentinal tubules (34). By using the CLSM method combined with computational analysis, we were able to assess spatially the killing performance of the IO-NP/H<sub>2</sub>O<sub>2</sub> compared to other modalities. PI is cell-impermeant and only enters bacterial cells with damaged membranes labelling dying or dead cell, but it does not measure cell vitality or metabolic activity. Having demonstrated the potential killing activity, further studies will focus on optimizing the nanoparticle formulation and detailing the effects on cell vitality using fluorescence probes for metabolic activity with PCR-based method for viable cell quantification (35).

## CONCLUSION

Altogether, our study reports a potentially new therapeutic approach for endodontic disinfection using the nanocatalysis concept for enhanced bacterial killing across the dentinal tubule. Iron oxide is a sustainable and biocompatible material that can be synthesized on large-scale using simple chemical synthesis methods at low cost, and currently used in FDA-approved formulations for chronic treatment (16). The flexibility of iron oxide chemistry allows the production of new nanoparticle shapes and sizes that may further improve catalytic activity (possibly with lower H<sub>2</sub>O<sub>2</sub> concentration) with enhanced dentinal tubules penetration. The efficacy of IO-NP/H<sub>2</sub>O<sub>2</sub> system should be further validated using animal models and in clinical studies that could lead to more effective and efficient endodontic treatment.

## ACKNOWLEDGEMENT

We are thankful to Dr. Brenda Gomes from State University of Campinas for providing the test organism *E. faecalis* OG1RF. The authors deny any conflicts of interest related to this study. The study was funded in part by the National Institute for Dental and Craniofacial Research grant DE025848.

The study was funded in part by the National Institute for Dental and Craniofacial Research grant DE025220.

## REFERENCES

- 1 ). Kakehashi S, Stanley HR, Fitzgerald RJ. The effects of surgical exposures of dental pulps in germ-free and conventional laboratory rats. *Oral Surg Oral Med Oral Pathol* 1965;20:340–9. [PubMed: 14342926]

- 2 ). Sjogren U, Figdor D, Persson S, Sundqvist G. Influence of infection at the time of root filling on the outcome of endodontic treatment of teeth with apical periodontitis. *Int Endod J* 1997;30:297–306. [PubMed: 9477818]
- 3 ). Trope M, Bergenholtz G. Microbiological basis for endodontic treatment: Can a maximum outcome be achieved in one visit. *EndodTopics* 2002;1:40–53.
- 4 ). Ramachandran Nair PN. Light and electron microscopic studies of root canal flora and periapical lesions. *J Endod* 1987;1:29–39.
- 5 ). Tronstad L, Barnett F, Cervone F. Periapical bacterial plaque in teeth refractory to endodontic treatment. *Endod Dent Traumatol* 1990;6:73–7. [PubMed: 2132213]
- 6 ). Andreasen JO, Rud J. A histobacteriologic study of dental and periapical structures after endodontic surgery. *Int J Oral Surg* 1972;1:272–81. [PubMed: 4199173]
- 7 ). Ando N, Hoshino E. Predominant obligate anaerobes invading the deep layers of root canal dentin. *Int Endod J* 1990;23:20–7. [PubMed: 2391177]
- 8 ). Haapasalo M, Shen Y. Current therapeutic options for endodontic biofilms. *Endod Topics* 2012;22:79–98.
- 9 ). Peters OA, Schonenberger K, Laib A. Effects of four Ni-Ti preparation techniques on root canal geometry assessed by micro computed tomography. *Int Endod J* 2001b;34:221–30. [PubMed: 12193268]
- 10 ). Paque F, Ganahl D, Peters OA. Effects of root canal preparation on apical geometry assessed by micro-computed tomography. *J Endod* 2009;35:1056–9. [PubMed: 19567334]
- 11 ). Heling I, Chandler NP. Antimicrobial effect of irrigant combinations within dentinal tubules. *Int Endod J* 1998;31:8–14. [PubMed: 9823123]
- 12 ). Wang Z, Shen Y, Haapasalo M. Effectiveness of endodontic disinfecting solutions against young and old *Enterococcus faecalis* biofilms in dentin canals. *J Endod* 2012;38:1376–9. [PubMed: 22980181]
- 13 ). Shrestha A, Kishen A. Antibacterial nanoparticles in endodontics: A review. *J Endod* 2016;42:1417–26. [PubMed: 27520408]
- 14 ). Samiei M, Farjami A, Dizaj SM, Lotfipour F. Nanoparticles for antimicrobial purposes in Endodontics: A systematic review of in vitro studies. *Material science and engineering* 2015;58:1269–78.
- 15 ). Shrestha A, Kishen A. Antibiofilm efficacy of photosensitizer-functionalized bioactive nanoparticles on multispecies biofilm. *J Endod* 2014;40:1604–10. [PubMed: 25260731]
- 16 ). Gao L, Liu Y, Kim D, Li Y, Hwang G, Naha PC, Cormode DP, Koo H. Nanocatalysts promote *Streptococcus mutans* biofilm matrix degradation and enhance bacterial killing to suppress dental caries in vivo. *Biomaterials* 2016;101:272–84. [PubMed: 27294544]
- 17 ). Basrani B, Haapasalo M. Update on endodontic irrigating solutions. *Endod Topics* 2012;27:74–102.
- 18 ). Noyori R, Aoki M, Sato K. Green oxidation with aqueous hydrogen peroxide, *Chem. Commun* 2003;16:1977–86.
- 19 ). Ricucci D, Siqueira JF, Jr., Bate AL, Pitt Ford TR. Histologic investigation of root canal-treated teeth with apical periodontitis: a retrospective study from twenty-four patients. *J Endod* 2009;35:493–502. [PubMed: 19345793]
- 20 ). Peters LB, Wesselink PR, Buijs JF, van Winkelhoff AJ. Viable bacteria in root dentinal tubules of teeth with apical periodontitis. *J Endod* 2001a;27:76–81. [PubMed: 11491642]
- 21 ). Matsuo T, Shirakami T, Ozaki K, Nakanishi T, Yumoto H, Ebisu S. An immunohistological study of the localization of bacteria invading root pulpal walls of teeth with periapical lesions. *J Endod* 2003;29:194–200. [PubMed: 12669880]
- 22 ). Haapasalo M, Shen Y, Qian W, Gao Y. Irrigation in endodontics. *Dent Clin North Am* 2010;54:291–312. [PubMed: 20433979]
- 23 ). Bystrom A, Sundqvist G. The antibacterial action of sodium hypochlorite and EDTA in 60 cases of endodontic therapy. *Int Endod J* 1985;18:35–40. [PubMed: 3922900]



- 24 ). Vianna ME, Horz HP, Gomes BP, Conrads G. In vivo evaluation of microbial reduction after chemo-mechanical preparation of human root canals containing necrotic pulp tissue. *Int Endod J* 2006;39:484–92. [PubMed: 16674744]
- 25 ). Gao L, Zhuang J, Nie L, Zhang J, Zhang Y, Gu N, Wang T, Feng J, Yang D, Perrett S, et al. Intrinsic peroxidase-like activity of ferromagnetic nanoparticles. *Nat Nanotechnol* 2007;2:577–83. [PubMed: 18654371]
- 26 ). Lopes MB, Sinhoreti MA, Gonini Junior A, Consani S, McCabe JF. Comparative study of tubular diameter and quantity for human and bovine dentin at different depths. *Braz Dent J* 2009;20:279–83. [PubMed: 20069249]
- 27 ). Moghadas L, Shahmoradi M, Narimani T. Antimicrobial activity of a new nanobased endodontic irrigation solution: in vitro study. *Dent. Hypotheses* 2012;3:142–6
- 28 ). Wu D, Fan W, Kishen A, Gutmann JL, Fan B. Evaluation of the antibacterial efficacy of silver nanoparticles against *Enterococcus faecalis* biofilm. *J Endod* 2014;40:285–90. [PubMed: 24461420]
- 29 ). Gomes BP, Pinheiro ET, Jacinto RC, Zaia AA, Ferraz CC, Souza-Filho FJ. Microbial analysis of canals of root-filled teeth with periapical lesions using polymerase chain reaction. *J Endod* 2008;34:537–40. [PubMed: 18436030]
- 30 ). Haapasalo M, Orstavik D. In vitro infection and disinfection of dentinal tubules. *J Dent Res* 1987;66:1375–9. [PubMed: 3114347]
- 31 ). Chavez de Paz LE, Bergenholtz G, Dahlen G, Svensater G. Response to alkaline stress by root canal bacteria in biofilms. *Int Endod J* 2007;40:344–55. [PubMed: 17326786]
- 32 ). Shin SJ, Jee SW, Song JS, Jung IY, Cha JH, Kim E. Comparison of regrowth of *Enterococcus faecalis* in dentinal tubules after sealing with gutta-percha or Resilon. *J Endod* 2008;34:445–8. [PubMed: 18358893]
- 33 ). Park E, Shen Y, Haapasalo M. Irrigation of the apical root canal. *Endod Topics* 2012;27:54–73
- 34 ). Zapata RO, Moraes IG, Bernardineli N, et al. Confocal laser scanning microscopy is appropriate to detect viability of *Enterococcus faecalis* in infected dentin. *J Endod* 2008;34:1198–201. [PubMed: 18793919]
- 35 ). Klein MI, Scott-Anne KM, Gregoire S, Rosalen PL, Koo H. Molecular approaches for viable bacterial population and transcriptional analyses in a rodent model of dental caries. *Mol Oral Microbiol* 2012;5:350–61

### Highlights

- In this study, we explore a new disinfection technology using biomimetic iron oxide nanoparticles with peroxidase-like activity that activates hydrogen peroxide catalysis for enhanced antibacterial activity using an in vitro infection model.
- Iron oxide nanoparticles when used as an irrigant together with hydrogen peroxide was significantly more effective in dentine disinfection in comparison with conventional endodontic irrigants such as sodium hypochlorite and chlorhexidine.
- Our results reveal the potential to exploit nanocatalysts with enzyme-like activity as a potent alternative approach for conventional irrigants.

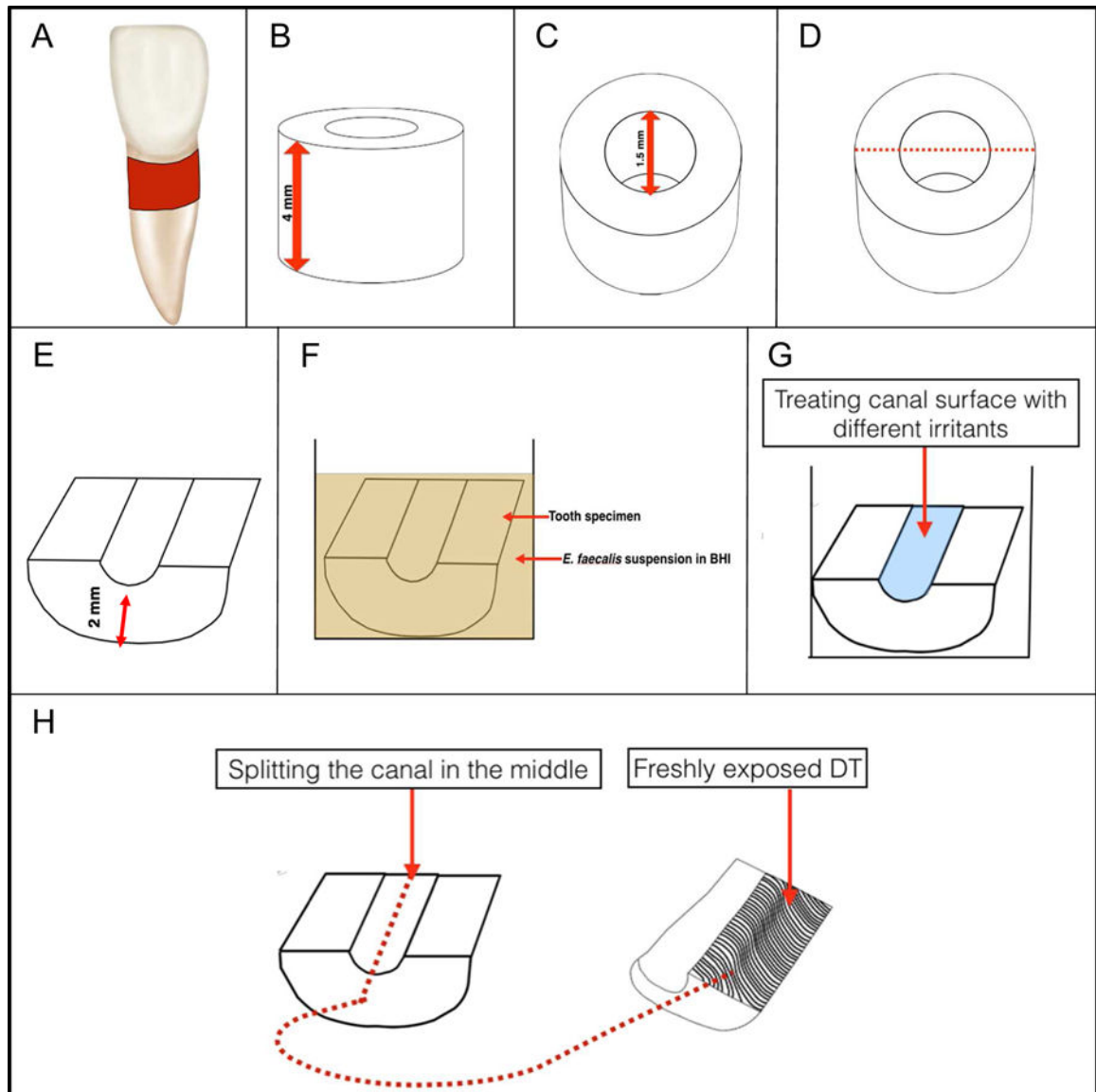


**Figure 1. Schematic diagram of root canal sample preparation.**

(A) Single rooted teeth; the area from which the dentin block is prepared marked with red. (B) Standardized 4 mm root dentin block. (C) Standardized root canal diameter preparation with size 6 Gates Glidden (1.5 mm diameter). (D) The vertical direction of block splitting into to semi cylindrical halves. (E) The outer surfaces of the semicylindrical halves (the cemental side) were ground to achieve a standard thickness of 2 mm and to remove the root surface cement. (F) The specimen was inoculated with an overnight suspension of *E. faecalis* in BHI (2 ml) adjusted spectrophotometrically to OD<sub>600</sub> of 0.5, which was grown for 3 weeks. (G) Disinfecting the sample with different control and test irrigants. (H) Splitting the canal surface to label freshly exposed DT with LIVE/DEAD BacLight staining and examine them under CLSM.

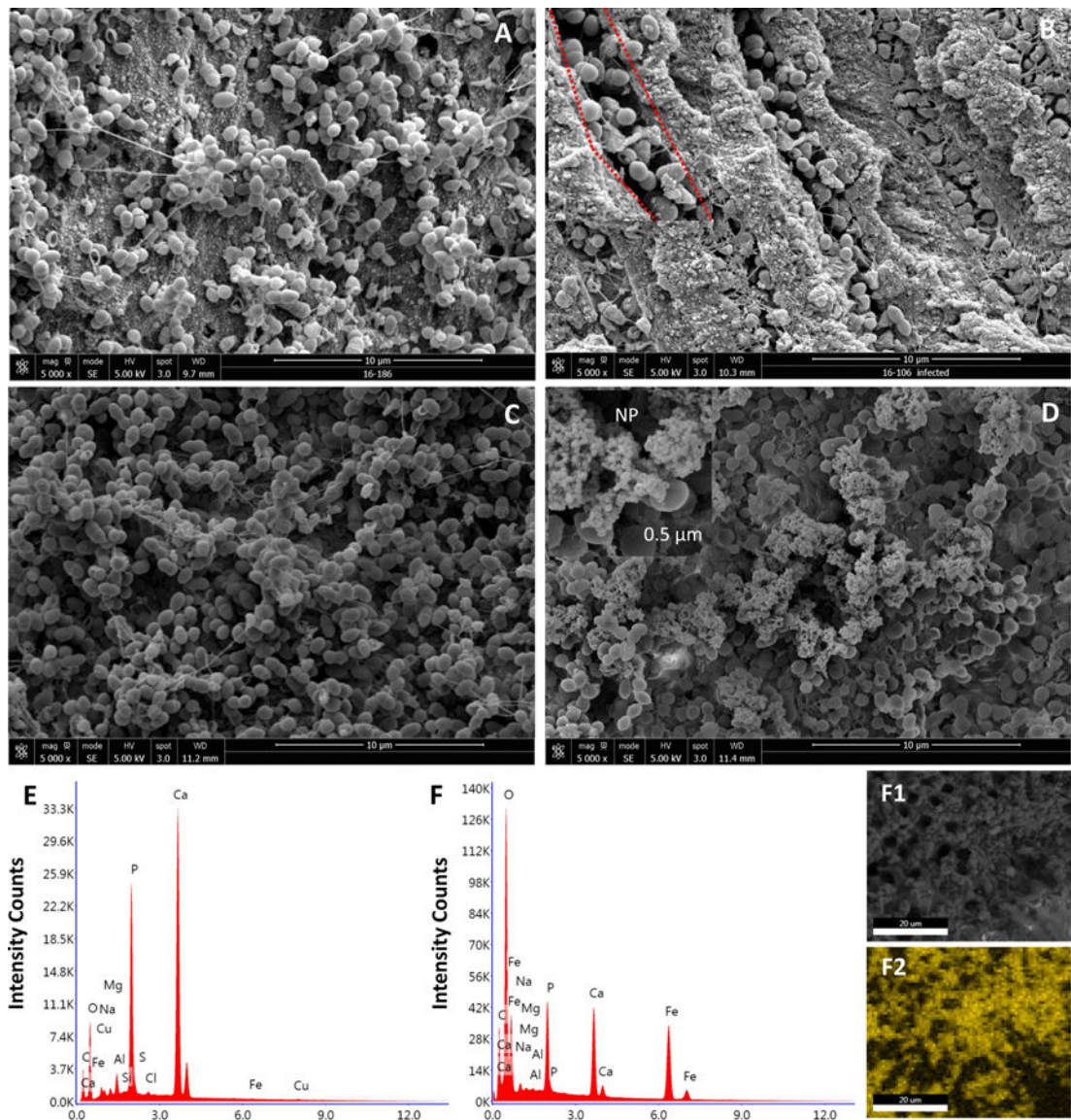


**Figure 2. SEM examination of biofilm formation, dentin infection and analysis of NP-treated and untreated surfaces.**

(A) Bacterial cluster typically found in biofilm structure attached to the dentinal wall of the canal surface at 5,000 X magnification (B) SEM micrograph showing heavily infected DT at 5,000 X magnification. At a higher magnification 10,000 X (the area marked by red) the morphology of enterococci can be visualized in detail. (C) An infected untreated specimen in which no NP were observed on the bacterial surfaces in comparison with (D) NP treated specimen. A closer look at the selected area, we observed small particles at nanometer scale (arrows) compared to the bacteria at microscale. (E, F) Elemental analysis showing the quantitative value of iron in NP treated sample (F) versus that of untreated sample (E). (F1,F2) Mapping out the NP using ESEM/EDS in which the yellow scale indicates the iron concentration, the brighter the pixel, the more concentrated the iron. The yellow color distribution (F2) correlates to the nanoparticles location in (F1).

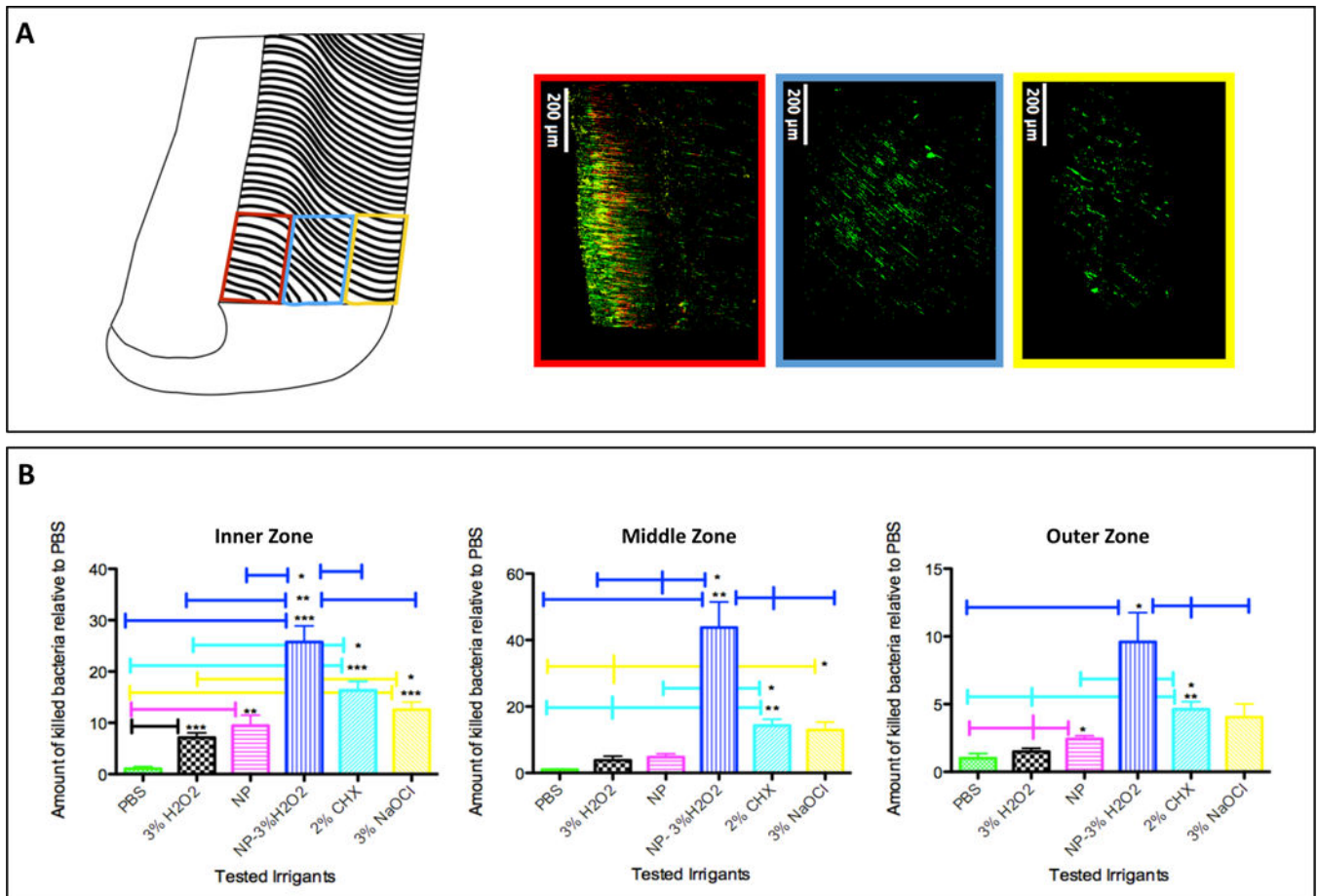


**Figure 3. Antibiofilm efficacy of IO-NP/H<sub>2</sub>O<sub>2</sub> disinfection system.**

(A) Schematic diagram illustrating the division of the split tooth surface into 3 zones. Inner (indicated by red), middle (blue) and outer (yellow) zones with representative CLSM images of dentinal tubules infected by *E. faecalis*. Samples were stained with LIVE/DEAD® BacLight™ Bacterial Viability kit (Molecular Probes, Eugene, OR) containing SYTO®9 green-fluorescent nucleic acid stain and the red-fluorescent nucleic acid stain, propidium iodide (PI). The representative image panels are color-coded corresponding to the zones indicated above (B) Quantitative analysis of CLSM imaging data. The amount of bacteria killed was measured by fold difference relative to PBS (negative control) at the inner zone, middle zone and outer zone. IO-NP/H<sub>2</sub>O<sub>2</sub> significantly killed more bacteria than either NP or H<sub>2</sub>O<sub>2</sub> alone and the other tested irrigants (CHX and NaOCl) in all zones (\*\*\* $P < .0005$ , \*\* $P < .005$  and \* $P < .05$ ).